Blackwell
Publishing

Full-length article

Design, synthesis and antitumor evaluation of a new series of *N*-substituted-thiourea derivatives[1]

Jian LI[2], Jin-zhi TAN[2], Li-li CHEN[2], Jian ZHANG[2], Xu SHEN[2,3], Chang-lin MEI[4,6], Li-li FU[4], Li-ping LIN[5], Jian DING[5], Bing XIONG[2], Xi-shan XIONG[4], Hong LIU[2,6], Xiao-min LUO[2,6], Hua-liang JIANG[2,3]

[2]*Drug Discovery and Design Centre, State Key Laboratory of Drug Research, Shanghai Institute of Materia Medica, Shanghai Institutes for Biological Sciences, Chinese Academy of Sciences, Shanghai 201203, China;* [3]*School of Pharmacy, East China University of Science and Technology, Shanghai 200237, China;* [4]*Division of Nephrology, Department of Internal Medicine, Changzheng Hospital, Second Military Medical University, Shanghai 200003, China;* [5]*Division of Antitumor Pharmacology, Shanghai Institute of Materia Medica, Shanghai 201203, China*

Key words

Abstract

Aim: To design and synthesize a novel class of protein tyrosine kinase inhibitors, featuring the *N*-(2-oxo-1,2-dihydroquinolin-3-yl-methyl)-thiourea framework. **Methods**: First, compounds 1 and 2 were identified using the virtual screening approach in conjunction with binding assay based on surface plasmon resonance. Subsequently, 3 regions of compounds 1 and 2 were selected for chemical modification. All compounds were characterized potent inhibitory activities toward the human lung adenocarcinoma cell line SPAC1. **Results**: Forty new compounds (1–2, 3a–g, 4a–w, and 5a–l) were designed, synthesized and bioassayed. Six compounds (1, 3e, 4l, 4w, 5a, and 5b) were found to show promising inhibitory activity against the SPAC1 tumor cell line. The inhibitory activity of compound 5a increases approximately 10 times more than that of the original compound 1. **Conclusion**: This study provides a promising new template with potential antitumor activity.

Introduction

Protein tyrosine kinases (PTK) play important roles in activating numerous signal transduction pathways within cells and are related to cellular proliferation, differentiation and various regulatory mechanisms[1,2]. Epidermal growth factor receptor (EGFR) is one of the important PTK. EGFR and its ligands (EGF and TGF-α) have been found to have high expression levels in many tumors of epithelial origin[1,3] and proliferative disorders of the epidermis, such as psoriasis[4]. Therefore, EGFR is an attractive target for the discovery of antitumor drugs[5–9].

EGFR has 3 domains: viz, an extracellular ligand binding domain; a single transmembrane domain; and an intracellular tyrosine kinase domain[10,11]. Although the receptor exists as an inactive monomer, dimerization takes place once it is activated by its ligands, resulting from the autophosphorylation of the intracellular tyrosine kinase domain[12]. Therefore, most of the reported inhibitors were designed by targeting the kinase domain of EGFR.

In the last decade, numerous small molecular inhibitors of EGFR have been reported[13–18], including 4-(phenylamino) quinazolines, 4-[ar(alk)ylamino]pyrido [4,3-*d*]pyrimidines, 4-(phenylamino)pyrrolo[2,3-*d*]pyrimidines, and 4-(phenyl-amino) pyrimido[5,4-*d*]pyrimidines[19,20]. Two selectively reversible EGFR inhibitors, ZD-1839 (Iressa)[21] and OSI-774 (Tarceva)[22], have been currently launched in the market. Despite the high potency and prolonged inhibition of EGFR

functions reported for some of these reversible inhibitors, the high intracellular concentrations of ATP make it difficult for inhibitors to reach sufficiently high concentrations *in vivo* to fully shut down EGF-stimulated signal transduction for long periods[23]. Some research groups[24,25] have therefore developed irreversible inhibitors based on the 4-(phenylamino)quinazolines, which can form a covalent bond with cysteines at the active site of the receptor by the Michael addition reaction.

Although EGFR inhibitors have exhibited curative effects in non-small cell lung cancer patients, some side effects with these agents have been sequentially found, such as cutaneous effects[26]. This thereby prompted us to discover novel EGFR inhibitors without serious side effects. In this paper, we presented a novel framework, which was identified by using a structure-based virtual screening approach[27–29] based on the crystal structure of OSI-774/EGFR-TK[30] in conjunction with chemical synthesis and bioassay. We hope that this research will provide a useful approach for the discovery of antitumor drugs.

Materials and methods

Virtual screening by molecular docking The crystal structure of EGFR-TK in complex with OSI-774 (PDB entry 1M17)[30] recovered from the Brookhaven Protein Data Bank was used as a target for virtual screening on the SPECS_1 database[31]. The DOCK 4.0 program (Kuntz group, San Francisco, CA, USA)[32,33] was employed for the primary screening. Residues of EGFR around OSI-774 at a radius of 5 Å were isolated for constructing the grids of the docking screening. The resulting substructure included all residues of the binding pocket. During the docking calculation, Kollman united-atom charges[34] were assigned to the protein, and Gasteiger-Marsili partial charges[35] were assigned to the small molecules in the SPECS_1 database. Conformational flexibility of the compounds from the database was considered during the docking search.

Three thousand molecules with the highest score obtained by DOCK search were rescored by using the Consensus Score method (CScore)[36,37] encoded in Sybyl6.8[38]. Molecules with a CScore of ≥4 were reevaluated by the pharmacophore[39] model of EGFR inhibitors.

Finally, 82 compounds were distinguished and purchased for bioassay on the basis of the above virtual screening flow. The virtual screening was performed on a 128-processor SGI Origin 3800 supercomputer (SGI, Mountain View, CA, USA).

Chemistry

Design of analogues of compounds 1 and 2 Com-
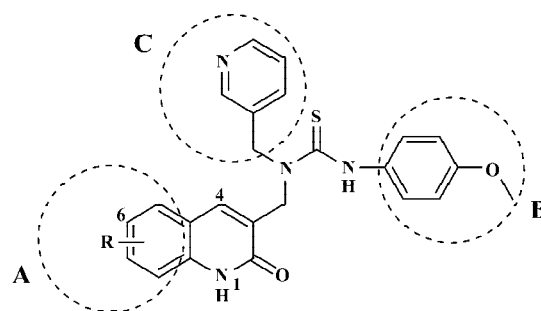
1: R=6-Me, K_D=1.46 µmol/L
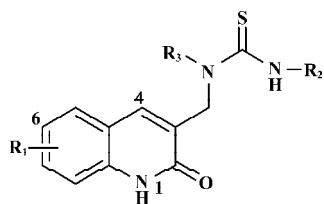**2: R**=7-Me, K_D=80.7 µmol/L

Figure 1. Structure of compounds 1–2, and 3 of their regions.

pounds 1–2 (Figure 1), bearing the higher binding affinities to EGFR as determined by the surface plasmon resonance (SPR) technology, were used as lead compounds to design new EGFR inhibitors. Having been kept the common moiety of compounds 1–2 of the *N*-(2-oxo-1,2-dihydro-quinolin-3-ylmethyl)-thiourea framework, 3 regions of these 2 molecules were selected to perform chemical modifications suitable to provide expedient and significant structure-activity relationship (SAR) information and improve inhibitory activity: (A) 6 or 7-Me substituent; (B) the *N'*-phenyl ring; and (C) the N-pyridinylmethyl side chain (Figure 1).

First, we used various steric electronic groups as substitute at positions 6, 7, and 8 of the 2-oxo-1,2-dihydro-quinoline ring in region A (Figure 1) and obtained 7 analogues (3a–g; Table 1). Second, by maintaining region A (6-Me or Br substituent) and replacing the 4-methoxyphenyl group in region B with other electronic and hydrophobic substituted aryl groups, we designed compounds 4a–w (Table 1). Finally, compounds 5a–h (Table 1) were achieved by replacing the pyridinylmethyl moiety in region C with electronic and hydrophobic groups.
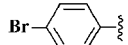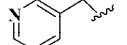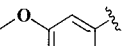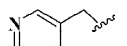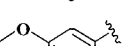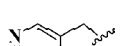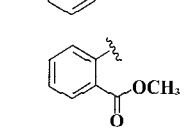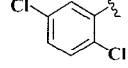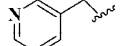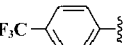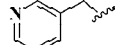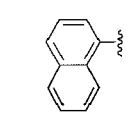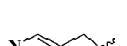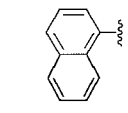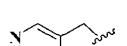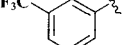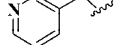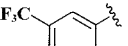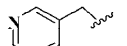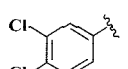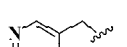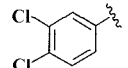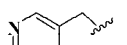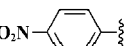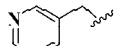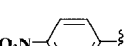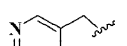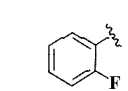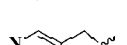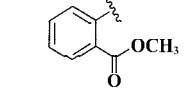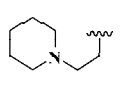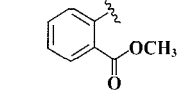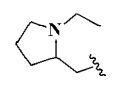
Synthetic procedures Figure 2 depicts the sequence of reactions that led to the preparation of compounds 1, 2, 3a–g, 4a–w, and 5a–h using *N*-aryl acetamide as the starting material. *N*-aryl acetamide reacted by refluxing with phosphoryl chloride in *N,N*-dimethylformamide (DMF), which afforded 2-chloro-quinoline-3-carbaldehyde 6[40]. Compound 6 was converted to the corresponding 2-oxo-1,2-dihydro-quinoline-3-carbaldehyde 7 by refluxing with hydrochloric acid[41,42]. Afterwards, 7 was condensed with various primary amines in ethanol and then was reduced with NaBH₄, giving the key intermediate 9. The target compounds 1, 4, 3a–g, 4a–w, and 5a–h (Table 1) were obtained by *N*-acylation of 9 using substituted isothiocyanates at room temperature.

Table 1. Chemical structures of compounds 1, 2, 3a–g, 4a–w, and 5a–h and their activity on enzyme and cell levels.

Compound	R_1	R_2	R_3	Biological assays	
				Enzyme assay[a] inhibition (%)	Tumor cell inhibition rate or IC_{50} (μmol/L)[b]
1	6-CH$_3$	4-methoxyphenyl	pyridin-3-ylmethyl	0	60.5
2	7-CH$_3$	4-methoxyphenyl	pyridin-3-ylmethyl	0	No inhibition at 50 μmol/L
3a	8-CH$_3$	4-methoxyphenyl	pyridin-3-ylmethyl	3.9	No inhibition at 50 μmol/L
3b	H	4-methoxyphenyl	pyridin-3-ylmethyl	0	11.8% inhibition at 50 μmol/L
3c	6-OCH$_3$	4-methoxyphenyl	pyridin-3-ylmethyl	8.4	20.4% inhibition at 50 μmol/L
3d	7-OCH$_3$	4-methoxyphenyl	pyridin-3-ylmethyl	6.8	8.4% inhibition at 50 μmol/L
3e	6-Br	4-methoxyphenyl	pyridin-3-ylmethyl	0	75.5
3f	7-Cl	4-methoxyphenyl	pyridin-3-ylmethyl	0	23.6% inhibition at 50 μmol/L
3g	6-CF$_3$	4-methoxyphenyl	pyridin-3-ylmethyl	0	18.4% inhibition at 20 μmol/L
4a	6-CH$_3$	3-chlorophenyl	pyridin-3-ylmethyl	2.6	19.1% inhibition at 20 μmol/L
4b	6-Br	3-chlorophenyl	pyridin-3-ylmethyl	3.7	2.3% inhibition at 20 μmol/L
4c	6-CH$_3$	4-methylphenyl	pyridin-3-ylmethyl	0	5.6% inhibition at 20 μmol/L
4d	6-Br	4-methylphenyl	pyridin-3-ylmethyl	0	2.4% inhibition at 20 μmol/L
4e	6-CH$_3$	4-(methylthio)phenyl	pyridin-3-ylmethyl	0	10.7% inhibition at 20 μmol/L
4f	6-Br	4-(methylthio)phenyl	pyridin-3-ylmethyl	7.5	3.1% inhibition at 20 μmol/L
4g	6-CH$_3$	4-(dimethylamino)naphthyl	pyridin-3-ylmethyl	0	No inhibition at 20 μmol/L
4h	6-CH$_3$	4-bromophenyl	pyridin-3-ylmethyl	0	12.7% inhibition at 20 μmol/L

(continue)

1261

Compound	R_1	R_2	R_3	Biological assays	
				Enzyme assay[a] inhibition (%)	Tumor cell inhibition rate or IC_{50} (μmol/L)[b]
4i	6-Br			6.4	13.0% inhibition at 20 μmol/L
4j	6-CH$_3$			0	5.3% inhibition at 20 μmol/L
4k	6-Br			0	8.4% inhibition at 20 μmol/L
4l	6-CH$_3$			0	43.8
4m	6-CH$_3$			0	20.1% inhibition at 20 μmol/L
4n	6-CH$_3$			2.8	16.2% inhibition at 20 μmol/L
4o	6-CH$_3$			0	5.1% inhibition at 20 μmol/L
4p	6-Br			0	5.1% inhibition at 20 μmol/L
4q	6-CH$_3$			4.2	12.2% inhibition at 20 μmol/L
4r	6-Br			7.5	9.2% inhibition at 20 μmol/L
4s	6-CH$_3$			0	15.7% inhibition at 20 μmol/L
4t	6-Br			0	5.1% inhibition at 20 μmol/L
4u	6-CH$_3$			9.1	17.9% inhibition at 20 μmol/L
4v	6-CH$_3$			13.0	No inhibition at 20 μmol/L
4w	6-CH$_3$			0	45.5
5a	6-CH$_3$			8.6	6.1
5b	6-CH$_3$			3.7	7.3

(continue)

Compound	R₁	R₂	R₃	Biological assays	
				Enzyme assay[a] inhibition (%)	Tumor cell inhibition rate or IC₅₀ (μmol/L)[b]
5c	6-CH₃	(methyl benzoate, OCH₃, O)	(indol-3-ylethyl)	0	36.1% inhibition at 20 μmol/L
5d	6-CH₃	(methyl benzoate, OCH₃, O)	(phenethyl)	0	26.0% inhibition at 20 μmol/L
5e	6-CH₃	(methyl benzoate, OCH₃, O)	(2-chlorophenethyl, Cl)	0	38.9% inhibition at 20 μmol/L
5f	6-CH₃	(methyl benzoate, OCH₃, O)	(thiophen-2-yl, S)	4.0	16.9% inhibition at 20 μmol/L
5g	6-CH₃	(methyl benzoate, OCH₃, O)	(furan-2-yl, O)	19.2	36.9% inhibition at 20 μmol/L
5h	6-CH₃	(methyl benzoate, OCH₃, O)	(benzodioxane, O, O)	4.7	12.0% inhibition at 20 μmol/L

[a] Inhibition percentage of kinase activity was generated by measuring the inhibition of phosphorylation of a peptide substrate added to the enzyme reaction in the presence of 10 μmol/L inhibitor.

[b] Human lung adenocarcinoma cell line SPAC1 with overexpressed EGFR. Dose-response curves were determined at 5 concentrations. IC₅₀ values are the concentrations in μmol/L needed to inhibit cell growth by 50% as determined from these curves.
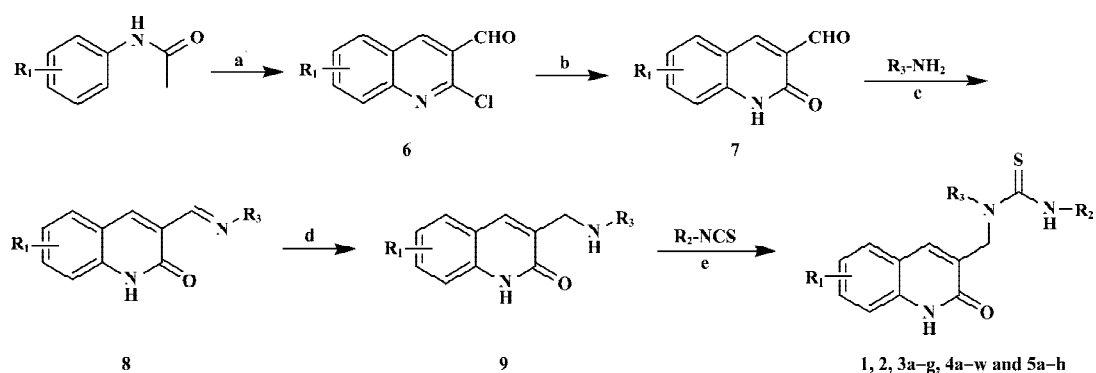
Figure 2. Reagents and conditions: (a) POCl₃, DMF; (b) 4 mol/L HCl, reflux; (c) ethanol, reflux; (d) NaBH₄, methanol; (e) toluene/methanol=15:1, 25 °C.

Surface plasmon resonance-based EGFR ligand binding assay

Construction of EGFR expression plasmid The coding sequence for EGFR was derived from a biologically active cDNA clone pRK5 (maintained in Shanghai Institute of Materia Medica). The EGFR coding region was amplified by the polymerase chain reaction (PCR) utilizing the forward primer with a sequence of 5'-ACTAGCATGCCAGGAGAGG-

GAGC-3' and a reverse primer 5'-CCGAAGCTTGTCTGTA-GGACT-3'. After digestion with *Sph* I and *Hind* III, the PCR product was inserted into the *Sph* I and *Hind* III sites of the vector pQE30 (Qiagen, Shanghai, China). The EGFR insert was verified by sequencing. The correct plasmid was transformed into the *Escherichia coli* M15 (*E coli* M15).

Expression and purification of EGFR *E coli* M15 cells transformed with the plasmid pQE30-EGFR were grown in LB medium containing ampicillin (100 μg/mL) and kanamycin (25 μg/mL) at 37 ºC overnight and then inoculated into 1 L fresh antibiotic-containing broth. The expression of EGFR was induced by the addition of 0.5 mmol/L of isopropyl β-*D*-thiogalactoside with further incubation for 6 h at 20 °C. The cell pellet was harvested by centrifugation at 4 °C, washed using 30 mL of 50 mmol/L Tris-HCl and 150 mmol/L NaCl (pH 8.0), rapidly frozen and stored at -70 °C until protein isolation was evident. The pellet was then disrupted by sonication against the buffer (20 mmol/L Tris-HCl and 0.5 mol/L NaCl; pH 8.0). The lysed cells were centrifuged at 10 621×*g* and stored at 4 ºC for 30 min. The supernatant was then discarded and the pellet was kept for refolding. The cell debris was solubilized using 2 mol/L urea and centrifuged at 10 621 ×*g* and stored at 4 ºC for 30 min. Semi-pure protein aggregates were resolubilized using 8 mol/L urea. The solubilized proteins were then refolded into their native state by dialysis against 500 volumes buffer (20 mmol/L Tris-HCl, 250 mmol/L NaCl, 0.5% NP-40, 0.4 mmol/L PMSF, 5.0 mmol/L reduced glutathione, 2.0 mmol/L oxidized glutathione and 100 mmol/L EDTA) and subsequently dialyzed against buffer A (20 mmol/L Tris-HCl, 0.5 mol/L NaCl and 10 mmol/L imidazole; pH 8.0). A 1-mL HiTrap Ni^{2+} chelating column was equilibrated with 10 mL of sterile deionized water, 50 mmol/L NiSO$_4$, and finally, 10 mL buffer A. The supernatant was passed over the column at a flow rate of 5 mL/min, followed by washing with 20 mL buffer A and 20 mL buffer B (80 mmol/L Tris-HCl, 0.5 mol/L NaCl and 80 mmol/L imidazole; pH 8.0), respectively. The protease of interest was eluted with 10 mL buffer C (20 mmol/L Tris-HCl, 0.5 mol/L NaCl and 0.5 mol/L imidazole; pH 8.0). The bioactivity of the highly purified His-tagged EGFR protein was measured using the protein tyrosine kinase assay kit (Chemicon, Temecula, CA, USA) and the concentration was measured with a UV spectrometer.

Binding assay The binding affinities of the virtual screening candidates to EGFR *in vitro* were determined by employing SPR technology. The measurement was performed using the dual flow cell Biacore 3000 instrument (Biacore AB, Uppsala, Sweden). Immobilization of the EGFR to the hydrophilic carboxymethylated dextran matrix of the sensor chip CM5 (Biacore, Sweden) was carried out by the standard primary amine coupling reaction wizard. In order for the EGFR to be covalently bound to the matrix, it was diluted in 10 mmol/L sodium acetate buffer (pH 4.2) to a final concentration of 0.025 mg/mL. Equilibration of the baseline was completed by a continuous flow of HBS-EP running buffer (10 mmol/L Hepes, 150 mmol/L NaCl, 3.4 mmol/L EDTA and 0.005% (*v/v*) surfactant P$_{20}$; pH 7.4) through the chip for 1–2 h. All the Biacore data were collected at 25 °C with HBS-EP as the running buffer at a constant flow of 30 μL/min. All the sensorgrams were processed by using automatic correction for non-specific bulk refractive index effects. The equilibrium constants (K_D values) evaluating the protein-ligand binding affinities were determined by the steady state affinity fitting analysis of the Biacore data.

Tyrosine kinase assays by ELISA The tyrosine kinase assays were previously measured using ELISA assay[43]. The tyrosine kinase activities of the purified EGFR were determined in 96-well ELISA plates pre-coated with 20 μg/mL poly (Glu, Tyr)$_{4:1}$ (Sigma Chemical Co, St Louis, MO, USA). Briefly, 85 μL of 8 μmol/L ATP solution diluted in kinase reaction buffer solution (50 mmol/L Hepes, pH 7.4, 20 mmol/L MgCl$_2$, 0.1 mmol/L MnCl$_2$, 0.2 mmol/L Na$_3$VO$_4$ and 1 mmol/L dithiothreitol (DTT) was added to each well. Then, 10 μL of diluted compounds were added to each reaction well at varying concentrations. 0.1% DMSO (*v/v*) was used as the negative control. Experiments at each concentration were performed in triplicate. The kinase reaction was initiated by the addition of purified tyrosine kinase proteins diluted in 10 μL of kinase reaction buffer solution. After incubation for 60 min at 37 °C, the plate was washed 3 times with PBS containing 0.1% Tween 20 (T-PBS). Next, 100 μL anti-phosphotyrosine (PY99) antibody (1:500 dilution) diluted in T-PBS containing 5 mg/mL bovine serum albumin (BSA) was added. After 30 min incubation at 37 °C, the plate was washed 3 times. Goat anti-mouse IgG horseradish peroxidase (100 μL; 1:2000 dilution) diluted in T-PBS containing 5 mg/mL BSA was added. The plate was reincubated at 37 °C for 30 min and washed as before. Finally, 100 mL solution (0.03% H$_2$O$_2$ and 2 mg/mL *o*-phenylenediamine in 0.1 mol/L citrate buffer; pH 5.5) was added and incubated at room temperature until color emerged. The reaction was terminated by the addition of 100 μL of H$_2$SO$_4$ (2 mol/L), and A_{492} was measured using a multiwell spectrophotometer (VERSAmax^{TM}, Charlot-tesville, VA, USA). The inhibition rate (IR; %) was calculated using Equation 1.

$$IR = (1 - A_{492}/A_{492control}) \times 100\% \qquad (1)$$

Cytotoxicity assay Human lung adenocarcinoma cell line SPCA1 with overexpressed EGFR, which was provided by Shanghai Institute of Cancer Research (Shanghai, China),

was used for the cell proliferation assay. The cells were cultivated in DMEM/F12 (Gibco, Langley, OK, USA) supplemented with 100 mL/L fetal calf serum (FCS; Sijiqing, Hangzhou, China), penicillin (100 mg/L) and streptomycin (100 mg/L) in a humidified atmosphere of 5% CO_2 at 37 °C.

The growth inhibition was evaluated by the modified MTT assay[44]. Briefly, the cells were seeded at 1×10^4 cells/well in 96-well plates (Falcon, CA, USA), and incubated for 24 h in 100 μL culture media with 10% FCS. The media were then replaced by serum-free medium. After 24 h, the media were placed in triplicate with grade concentrations of compounds. As controls, the cells were cultivated in DMEM/F12 only. The cells were then treated by MTT (Sigma, USA) assay, 10 μL (5 g/L) for 4 h. After the removal of the supernatant, the purple-blue sediment was dissolved in 100 μL/well DMSO, and the optical densities were read on the multi-well scanning spectrophotometer (Labsystems Dragon, Finland) at 490 nm (A_{490}). The growth inhibition rate (GIR) of the treated cells was calculated using Equation 2:

$$GIR(\%) = \{1 - [A_{490}/A_{490}(control)]\} \times 100\% \qquad (2)$$

The results were also converted to IC_{50} (the compound concentration required for 50% growth inhibition of tumor cells), which were calculated by using the sigmoidal fitting model by the Origin 7.0 software (OriginLab, Northampton, MA, USA). The mean IC_{50} was determined from the results of 3 independent tests.

Results

Lead identification by virtual screening and binding assay Targeting the crystal structure of EGFR (PDB entry 1M17)[30], we searched the SPECS_1 database by using the DOCK 4.0 program[32,33]. The small molecules were ranked according to their scores calculated by using the scoring function of DOCK. The top 3000 candidate molecules were obtained with the best scores by a shape complementarity scoring function in DOCK[32,33]. These compounds were re-estimated using Cscore[36,37]. The compounds with a Cscore=4 or 5 (the best score of Cscore is 5) were subsequently evaluated again using the pharmacophore[39] model of EGFR inhibitors. Finally, 82 compounds were selected according to the criterion of pharmacophore for biological assay. Because enzymatic assay is time consuming, therefore, SPR measurements were used for the primary screening, determining the binding affinity of these 82 candidate molecules to EGFR. Immobilization of EGFR resulted in a resonance signal at about 10 000 resonance units (RU). Among the 82 compounds, the biosensor RU of 26 compounds were concentration dependent. The collected data indicated that these 26 compounds (including compounds 1–2) can bind to EGFR

in vitro and the binding affinities to EGFR are in the submicro or micromolar range (K_D=97.7–0.39 μmol/L). These compounds could be designated as binders (or hits) of EGFR. Chemical structures and binding affinities of compounds 1 and 2 are shown in Figure 1.

Analogs design and synthesis On the basis of the framework of compounds 1 and 2, 38 compounds (3a–g, 4a–w, and 5a–l) were designed and synthesized; their chemical structures are shown in Table 1. These compounds were synthesized through the route outlined in Figure 2, and the details for synthetic procedures and structural characterizations have been previously described.

Inhibitory activity towards tyrosine kinase We also evaluated EGFR kinase inhibitory activity of designed compounds using kinase autophosphorylation assay by ELISA (Table 1). Disappointingly, most compounds just displayed low inhibition against the autophosphorylation of EGFR kinase at a concentration of 10 μmol/L. The enzymatic activities of the compounds 1 and 2 do not consistently correlate with the SPR-binding affinities. The reason may be that the protein was immobilized to a sensor chip in the SPR assay, which affects the conformational flexibility of the protein. Compounds 1 and 2 are good binders and moderate inhibitors to EGFR. Accordingly, the effects of compounds on tumor cell activity were determined.

Inhibition activity against the proliferation of tumor cells Cell growth inhibitory activities on SPCA1 cell of the 40 inhibitors (1–2, 3a–g, 4a–w, and 5a–h) were evaluated. The results are listed in Table 1 and indicate that compounds 1, 3e, 4l, 4w, 5a, and 5b show potent inhibitory influence on the viability of the SPCA1. It is remarkable that the inhibitory activity of compound 5a increases approximately 10 times more than that of compound 1. These encouraging results prove the validity of our chemical modification.

Discussion

According to the above results (Table 1), we can draw some noteworthy conclusions: (1) 6-substitutions on the quinoline ring in region A (Table 1) is favorable for maintaining activity, especially within small groups (eg, compound 1); (2) 2-monosubstitutions on the phenyl ring in region B (Table 1) can substantially improve potency. Replacement of the phenyl ring with the large naphthanyl ring cannot be tolerated, nearly leading to a loss of activity. Thus, compounds 4l and 4w are more potent than compounds 4a–4k and 4m–4v; and (3) the introduction of the cycloalkyl moiety (5a–b) in region C (Table 1) improves activity distinctly compared with the (hetero) aromatic moiety (5c–h).

The inconsistency between enzyme activity and cellular

efficiency was explained tentatively based on the docking simulation. We compare the 3D binding models of OSI-774[30] to EGFR obtained from the crystal structure with that of compound 5a to EGFR generated based on the docking simulation (Figure 3). Figure 3A shows that the nitrogen (N1) of the quinazoline of OSI-774 accepts a hydrogen-bond (H-bond) from the amide nitrogen of Met769, simultaneously; the other quinazoline nitrogen (N3) forms a strong H bond interaction with the Thr766 side chain through a water molecule bridge, which is important for maintaining inhibitory activity[30,45]. Whereas the N1 of the quinoline moiety of 5a forms a H-bond with the backbone carbonyl group of Met769, the phenyl ring in the B region and the piperidine ring in C region form weak hydrophobic interactions with residues Leu694, Val702, Leu820, and Thr830 (Figure 3B). The above difference in the formation of H-bonds between the inhibitors and the kinase domain may affect the inhibition of EGFR kinase activity. This indicates that our designed compounds might interact with multiple proteins involved in the EGFR signaling pathways[16] and not only target the tyrosine kinase, thus leading to the promising antiproliferation effect against the SPAC1 cell line.

In summary, six potent compounds (1, 3e, 4l, 4w, 5a, and 5b) were discovered by using a structure-based virtual screening approach in conjunction with chemical synthesis and bioassay. Although the enzymatic assay showed that these 6 compounds just displayed low EGFR kinase inhibitory activity at the concentration of 10 μmol/L, the cellular assay indicated that they exhibited promising inhibitory activity toward the SPAC1 cell line. The preliminary SAR was obtained, which shows that 6 substitutions of the quinoline ring in the A region, the 2-substituted phenyl ring in the B region and the cycloalkyl moiety in the C region are essential for inhibitory activity against SPAC1. Meanwhile, the molecular modeling revealed that the introduction of the H-bond donor and/or acceptor atom to the phenyl ring part of the quinoline moiety would be likely to produce additional H-bond interactions, therefore enhancing molecular bioactivity. In addition, compounds 5a–b with tertiary aliphatic amines in the side chain, show potent antiproliferation activity. Remarkably, compound 5a showed inhibitory capability approximately 10 times higher than that of the prototype compound 1, demonstrating that the chemical modification strategy employed in this study is efficient and valuable for further structural modification.

Appendix

The reagents (chemicals) were purchased from Lancaster (Morecambe, England), Acros (Geel, Belgium) and Shanghai Chemical Reagent Company (Shanghai, China), and were used without further purification. The analytical thin-layer chromatography was HSGF 254 (150–200 μm thickness; Yantai Huiyou Company, Yantai, Shandong, China). Yields were not optimized. Melting points were measured in a capillary tube on a SGW X-4 melting point apparatus without correction. Nuclear magnetic resonance (NMR) spectra were given on a Brucker AMX-400 and AMX-300 (Brucker, Fällanden, Switzerland; internal standard as tetramethylsilane). Chemical shifts were reported in parts per million (ppm, δ) downfield from tetramethylsilane. Proton coupling patterns were described as singlet (s), doublet (d), triplet (t), quartet (q), multiplet (m), and broad (br). Low- and high-resolution (HRMS) mass spectra were given with an electric ionization and electrospray (EI, ESI) and a LCQ-DECA spectrometer produced by Finnigan MAT-95 (Finnigan, Santa Clara, CA, USA).
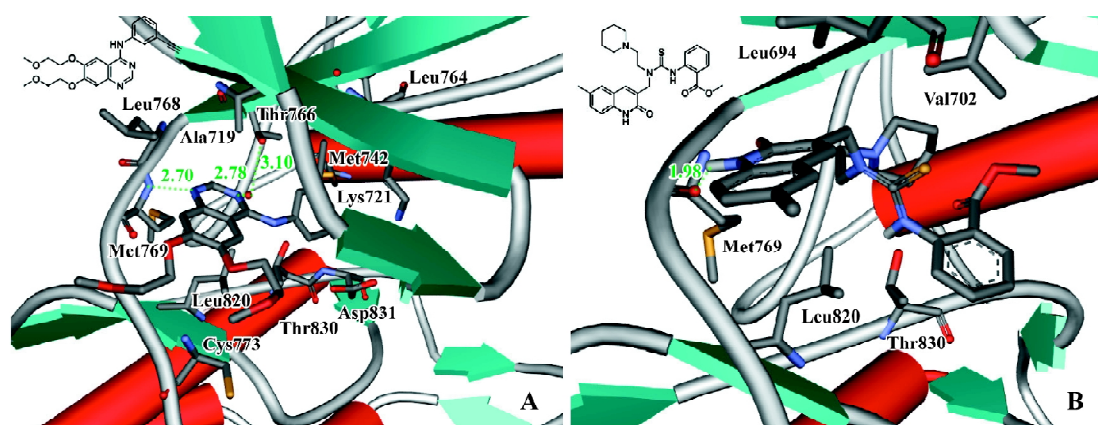

Figure 3. Binding models of OSI-774 (A) and 5a (B) at the ligand binding site of EGFR. The H-bond is represented by the green dotted line. This picture was prepared using ViewerPro (http://www.accelrys.com/).

General procedures for the preparations of 7[40–42] are described as those for 2-oxo-1,2-dihydro-quinoline-3-carbaldehyde (7a) DMF (4.8 mL, 0.0625 mol) was added to phosphoryl chloride (16.1 mL, 0.175 mol) dropwise, stirred at 0 °C before adding the *N*-phenyl acetamide (3.375 g, 0.025 mol). After 5 min, the mixture was heated at 75 °C for 16 h. On pouring the reaction mixture into ice water, the precipitate was filtrated to afford 2-chloro-quinoline-3-carbaldehyde (6a) (3.1 g, 64%) as a yellow solid; mp 144–146 °C (lit[40] 148–149 °C); EI-MS *m/z* 191 (M+).

A mixture of 6a (3.1 g) and aqueous hydrochloric acid (55 mL; 4 mol/L) was heated under reflux for 1 h, and then allowed to cool in ice and filtered to afford 2-oxo-1,2-dihydro-quinoline-3-carbaldehyde (7a) (2.6 g, 92%) as a yellow solid; mp 300 °C (lit[34] 298 °C); EI-MS *m/z* 173 (M+).

General procedures for the preparation of 9 are described as those for 3-{[(pyridin-3-ylmethyl)-amino]-methyl}-1*H*-quinolin-2-one (9a) A mixture of 2-oxo-1,2-dihydro-quinoline-3-carbaldehyde (7a) (0.5 g, 2.9 mmol), pyridin-3-yl-methylamine (0.31 g, 2.9 mmol), and ethanol (50 mL) were refluxed while stirred for 12 h. The reaction mixture was concentrated under reduced pressure to approximately 10 mL and then allowed to cool in ice and filtered to afford 3-[(pyridin-3-ylmethylimino)-methyl]-1*H*-quinolin-2-one 8a (0.6 g, 78%) as a yellow solid; mp 180–182 °C; ^{1}H NMR (DMSO-d$_6$, 400 MHz): δ 4.87 (s, 2H), 7.21 (dt, 1H, J=7.6 and 1.2 Hz), 7.33 (d, 1H, J=8.4 Hz), 7.39 (ddd, 1H, J=7.6, 4.8 and 0.8 Hz), 7.56 (dt, 1H, J=7.6 and 1.2 Hz), 7.76 (td, 1H, J=8.0 and 2.0 Hz), 7.83 (dd, 1H, J=8.0 and 1.2 Hz), 8.49 (m, 2H), 8.59 (d, 1H, J=2.0 Hz), 8.74 (t, 1H, J=1.6 Hz). EI-MS *m/z* 263 (M+).

A mixture of 8a (0.11 g, 0.38 mmol), NaBH$_4$ (0.038 g, 1 mmol) and methanol (5 mL) was stirred at rt for 1 h, poured into H$_2$O (30 mL) and extracted with CHCl$_3$. The combined organic layer was dried, filtered and condensed under reduced pressure. The residue was washed with a mixture of EtOAc/petroleum ether (1:1, *v/v*) to afford 9a (0.095 g, 85%) as a yellow solid; mp 151–153 °C; ^{1}H NMR (DMSO-d$_6$, 400 MHz): δ 2.78 (br, 1H, NH), 3.55 (s, 2H), 3.85 (s, 2H), 7.16 (t, 1H, J=7.5 Hz), 7.29 (d, 1H, J=8.2 Hz), 7.35 (dd, 1H, J=7.7 and 4.8 Hz), 7.45 (t, 1H, J=7.7 Hz), 7.65 (d, 1H, J=7.2 Hz), 7.79 (d, 1H, J=7.7 Hz), 7.87 (s, 1H), 8.44 (dd, 1H, J=4.8 and 1.5 Hz), 8.55 (d, 1H, J=1.8 Hz), 11.78 (s, 1H, NHCO). EI-MS *m/z* 265 (M+)

General procedures for the preparation of N,N,N'-tri-substituted thiourea 1-5 are described as those for 3b. N'-(4-methoxyphenyl)-*N*-[(2-oxo-1,2-dihydro-3-quinolinyl)methyl]-*N*-(3-pyridinylmethyl)thiourea (3b) A mixture of 9a (55 mg, 0.207 mmol), 4-methoxyphenyl isothiocyanate (35 mg, 0.207 mmol), toluene (8 mL), and methanol (1 mL) was stirred for 24 h at rt, and then allowed to cool in ice and filtered, to afford 3b (71 mg, 80%) as an off-white solid; mp 179–181 °C; ^{1}H NMR (DMSO-d$_6$, 400 MHz): δ 3.73 (s, 3H), 4.67 (s, 2H), 5.21 (s, 2H), 6.90 (d, 2H, J=8.8 Hz), 7.25 (t, 1H, J=7.5 Hz), 7.30 (d, 2H, J=8.8 Hz), 7.36 (m, 2H), 7.55 (t, 1H, J=7.2 Hz), 7.72 (d, 1H, J=7.6 Hz), 7.80 (d, 1H, J=7.6 Hz), 7.90 (s, 1H), 8.44 (dd, 1H, J=4.7 and 1.6 Hz), 8.58 (d, 1H, J=1.9 Hz), 10.63 (s, 1H, NH), 12.29 (s, 1H, NH); ESI-MS *m/z* 453 [M+Na]+. HRMS (ESI) *m/z* calcd C$_{24}$H$_{22}$N$_4$O$_2$SNa [M+Na]+ 453.1361 found 453.1370.

N'-(4-Methoxyphenyl)-*N*-[(6-methyl-2-oxo-1,2-dihydro-3-quinolinyl)methyl]-*N*-(3-pyridinylmethyl)thiourea (1) A white solid, yield 73%; mp 220–222 °C; ^{1}H NMR (DMSO-d$_6$, 300 MHz): δ 2.34 (s, 3H), 3.73 (s, 3H), 4.64 (s, 2H), 5.19 (s, 2H), 6.91 (d, 2H, J=6.9 Hz), 7.25–7.38 (m, 5H), 7.51 (s, 1H), 7.81 (d, 1H, J=6.0 Hz), 7.84 (s, 1H), 8.44 (dd, 1H, J=4.6 and 1.4 Hz), 8.58 (d, 1H, =1.5 Hz), 10.75 (s, 1H, NH), 12.25 (s, 1H, NH); ESI-MS *m/z* 467 [M+Na]+. HRMS (ESI) *m/z* calcd C$_{25}$H$_{24}$N$_4$O$_2$SNa [M+Na]+ 467.1518 found 467.1519.

N'-(4-Methoxyphenyl)-*N*-[(7-methyl-2-oxo-1,2-dihydro-3-quinolinyl)methyl]-*N*-(3-pyridinylmethyl)thiourea (2) A pale yellow solid, yield 69%; mp 185–187 °C; ^{1}H NMR (DMSO-d$_6$, 300 MHz): δ 2.40 (s, 3H), 3.74 (s, 3H), 4.65 (s, 2H), 5.21 (s, 2H), 6.90 (d, 2H, J=8.8 Hz), 7.09 (d, 1H, J=8.0 Hz), 7.15 (s, 1H), 7.31 (d, 2H, J=8.8 Hz), 7.36 (dd, 1H, J=8.0 and 4.8 Hz), 7.62 (d, 1H, J=8.4 Hz), 7.81 (d, 1H, J=8.0 Hz), 7.89 (s, 1H), 8.44 (dd, 1H, J=4.8 and 1.6 Hz), 8.59 (d, 1H, J=1.5 Hz), 10.65 (s, 1H, NH), 12.20 (s, 1H, NH); ESI-MS *m/z* 445 [M+H]+. HRMS (ESI) *m/z* calcd C$_{25}$H$_{25}$N$_4$O$_2$S [M+H]+ 445.1698 found 445.1697.

N'-(4-Methoxyphenyl)-*N*-[(8-methyl-2-oxo-1,2-dihydro-3-quinolinyl)methyl]-*N*-(3-pyridinylmethyl)thiourea (3a) An off-white solid, yield 46%; mp 200–201 °C; ^{1}H NMR (DMSO-d$_6$, 300 MHz): δ 2.44 (s, 3H), 3.73 (s, 3H), 4.68 (s, 2H), 5.20 (s, 2H), 6.90 (d, 2H, J=8.8 Hz), 7.16 (t, 1H, J=7.6 Hz), 7.30 (d, 2H, J=8.8 Hz), 7.35 (dd, 1H, J=8.0 and 4.8 Hz), 7.39 (d, 1H, J=7.8 Hz), 7.56 (d, 1H, J=7.6 Hz), 7.80 (d, 1H, J=7.8 Hz), 7.90 (s, 1H), 8.43 (dd, 1H, J=4.8 and 1.6 Hz), 8.59 (d, 1H, J=2.0 Hz), 10.60 (s, 1H, NH), 11.45 (s, 1H, NH); ESI-MS *m/z* 467 [M+Na]+. HRMS (ESI) *m/z* calcd C$_{25}$H$_{24}$N$_4$O$_2$SNa [M+Na]+ 467.1518 found 467.1483.

N'-(4-Methoxyphenyl)-*N*-[(6-methoxy-2-oxo-1,2-dihydro-3-quinolinyl)methyl]-*N*-(3-pyridinylmethyl)thiourea (3c) A yellow solid, yield 66%; mp 207–209 °C; ^{1}H NMR (DMSO-d$_6$, 300 MHz): δ 3.75 (s, 3H), 3.81 (s, 3H), 4.65 (s, 2H), 5.20 (s, 2H), 6.91 (d, 2H, J=8.8 Hz), 7.21 (dd, 1H, J=9.2 and 2.4 Hz), 7.33 (m, 4H), 7.39 (dd, 1H, J=8.0 and 4.8 Hz), 7.84 (d, 1H, J=8.0 Hz), 7.91 (s, 1H), 8.48 (dd, 1H, J=4.8 and 1.6 Hz), 8.63 (d, 1H, J=2.0 Hz), 10.80 (s, 1H, NH), 12.23 (s, 1H, NH); ESI-MS *m/z* 461 [M+H]+. HRMS (ESI) *m/z* calcd C$_{25}$H$_{25}$N$_4$O$_3$S [M+H]+ 461.1647 found 461.1618.

N'-(4-Methoxyphenyl)-*N*-[(7-methoxy-2-oxo-1,2-dihydro-3-quinolinyl)methyl]-*N*-(3-pyridinylmethyl)thiourea (3d) A yellow solid, yield 58%; mp 189–191 °C; ^{1}H NMR (DMSO-d$_6$, 300 MHz): δ 3.74 (s, 3H), 3.82 (s, 3H), 4.62 (s, 2H), 5.20 (s, 2H), 6.91 (m, 4H), 7.37 (m, 3H), 7.66 (d, 1H, J=8.4 Hz), 7.81 (d, 1H, J= 8.4 Hz), 7.89 (s, 1H), 8.45 (dd, 1H, J=4.8 and 1.8 Hz), 8.59 (d, 1H, J=2.1 Hz), 10.48 (s, 1H, NH), 12.13 (s, 1H, NH); ESI-MS *m/z* 483 [M+Na]+. HRMS (ESI) *m/z* calcd C$_{25}$H$_{24}$N$_4$O$_3$SNa [M+Na]+ 483.1647 found 483.1459.

N'-(4-Methoxyphenyl)-*N*-[(6-bromo-2-oxo-1,2-dihydro-3-quinolinyl)methyl]-*N*-(3-pyridinylmethyl)thiourea (3e) A white solid, yield 55%; mp 233–235 °C; ^{1}H NMR (DMSO-d$_6$, 300 MHz): δ 3.73 (s, 3H), 4.66 (s, 2H), 5.18 (s, 2H), 6.89 (d, 2H, J=8.8 Hz), 7.25–7.30 (m, 3H), 7.37 (dd, 1H, J=7.6 and 4.8 Hz), 7.68 (dd, 1H, J=8.8 and 2.4 Hz), 7.81 (d, 1H, J=8.0 Hz), 7.84 (s, 1H), 8.03 (d, 1H, J=1.8 Hz), 8.45 (dd, 1H, J=4.8 and 1.6 Hz), 8.59 (d, 1H, J=2.0 Hz), 10.40 (s, 1H, NH), 12.40 (s, 1H, NH); ESI-MS *m/z* 531 [M+Na]+. HRMS (ESI) *m/z* calcd C$_{24}$H$_{21}$N$_4$O$_2$SBrNa [M+Na]+ 531.0466 found 531.0477.

N'-(4-Methoxyphenyl)-*N*-[(7-chloro-2-oxo-1,2-dihydro-3-quinolinyl)methyl]-*N*-(3-pyridinylmethyl)thiourea (3f) A pale yellow solid, yield 83%; mp 206–208 °C; ^{1}H NMR (DMSO-d$_6$, 300 MHz): δ 3.74 (s, 3H), 4.69 (s, 2H), 5.22 (s, 2H), 6.90 (d, 2H, J=8.8 Hz), 7.25–7.30 (m, 3H), 7.38 (m, 2H), 7.81 (m, 2H), 7.87 (s, 1H), 8.45 (dd, 1H, J=4.8 and 1.6 Hz), 8.59 (d, 1H, J=2.0 Hz), 10.38 (s, 1H,

NH), 12.30 (s, 1H, NH); ESI-MS *m/z* 487 [M+Na]⁺. HRMS (ESI) *m/z* calcd $C_{24}H_{21}N_4O_2SClNa$ [M+Na]⁺ 487.0971 found 487.1010.

***N'*-(4-Methoxyphenyl)-*N*-[(6-trifluoromethyl-2-oxo-1,2-dihydro-3-quinolinyl)methyl]-*N*-(3-pyridinylmethyl)thiourea (3g)** An off-white solid, yield 66%; mp 231–233 °C; ¹H NMR (DMSO-d₆, 300 MHz): δ 3.75 (s, 3H), 4.71 (s, 2H), 5.21 (s, 2H), 6.91 (d, 2H, J=8.8 Hz), 7.30 (d, 2H, J=8.8 Hz), 7.41 (dd, 1H, J=7.6 and 4.8 Hz), 7.52 (d, 1H, J=8.4 Hz), 7.86 (m, 2H), 8.00 (s, 1H), 8.28 (s, 1H), 8.48 (dd, 1H, J=4.8 and 1.6 Hz), 8.62 (d, 1H, J=1.6 Hz), 10.18 (s, 1H, NH), 12.52 (s, 1H, NH); ESI-MS *m/z* 521 [M+Na]⁺. HRMS (ESI) *m/z* calcd $C_{25}H_{21}N_4O_2SF_3Na$ [M+Na]⁺ 521.1235 found 521.1272.

***N'*-(3-Chlorophenyl)-*N*-[(6-methyl-2-oxo-1,2-dihydro-3-quinolinyl)methyl]-*N*-(3-pyridinylmethyl)thiourea (4a)** A white solid, yield 50%; mp 220–221 °C; ¹H NMR (DMSO-d₆, 300 MHz): δ 2.37 (s, 3H), 4.67 (s, 2H), 5.19 (s, 2H), 7.20 (d, 1H, J=6.0 Hz), 7.29–7.44 (m, 4H), 7.49 (d, 1H, J=8.1 Hz), 7.56 (s, 1H), 7.65 (t, 1H, J=2.0 Hz), 7.83 (d, 1H, J=8.1 Hz), 8.00 (s, 1H), 8.47 (dd, 1H, J=4.8 and 1.5 Hz), 8.62 (d, 1H, J=1.8 Hz), 10.59 (s, 1H, NH), 12.44 (s, 1H, NH); ESI-MS *m/z* 471 [M+Na]⁺. HRMS (ESI) *m/z* calcd $C_{24}H_{21}N_4OSClNa$ [M+Na]⁺ 471.1022 found 471.1028.

***N'*-(3-Chlorophenyl)-*N*-[(6-bromo-2-oxo-1,2-dihydro-3-quinolinyl)methyl]-*N*-(3-pyridinylmethyl)thiourea (4b)** A pale yellow solid, yield 46%; mp 229–231 °C; ¹H NMR (DMSO-d₆, 300 MHz): δ 4.68 (s, 2H), 5.19 (s, 2H), 7.21 (d, 1H, J=7.8 Hz), 7.32–7.41 (m, 3H), 7.48 (d, 1H, J=7.8 Hz), 7.62 (t, 1H, J=2.0 Hz), 7.74 (dd, 1H, J=8.7 and 2.1 Hz), 7.85 (d, 1H, J=7.8 Hz), 7.97 (s, 1H), 8.08 (d, 1H, J=2.4 Hz), 8.49 (dd, 1H, J=4.8 and 1.8 Hz), 8.63 (d, 1H, J=1.5 Hz), 11.04 (s, 1H, NH), 12.64 (s, 1H, NH); ESI-MS *m/z* 513 [M+H]⁺. HRMS (ESI) *m/z* calcd $C_{23}H_{19}N_4OSClBr$ [M+H]⁺ 513.0151 found 513.0152.

***N'*-(4-Methylphenyl)-*N*-[(6-methyl-2-oxo-1,2-dihydro-3-quinolinyl)methyl]-*N*-(3-pyridinylmethyl)thiourea (4c)** A white solid, yield 63%; mp 201–203 °C; ¹H NMR (DMSO-d₆, 300 MHz):δ 2.31 (s, 3H), 2.37 (s, 3H), 4.67 (s, 2H), 5.21 (s, 2H), 7.09 (m, 3H), 7.24-7.43 (m, 4H), 7.55 (s, 1H), 7.84 (d, 1H, J=7.8 Hz), 7.93 (s, 1H), 8.48 (dd, 1H, J=4.8 and 1.5 Hz), 8.62 (d, 1H, J=1.8 Hz), 11.12 (s, 1H, NH), 12.30 (s, 1H, NH); ESI-MS *m/z* 451 [M+Na]⁺. HRMS (ESI) *m/z* calcd $C_{25}H_{24}N_4OSNa$ [M+Na]⁺ 451.1569 found 451.1555.

***N'*-(4-Methylphenyl)-*N*-[(6-bromo-2-oxo-1,2-dihydro-3-quinolinyl)methyl]-*N*-(3-pyridinylmethyl)thiourea (4d)** An off-white solid, yield 49%; mp 230–232 °C; ¹H NMR (DMSO-d₆, 300 MHz): δ 2.30 (s, 3H), 4.69 (s, 2H), 5.21 (s, 2H), 7.17 (d, 2H, J=8.1 Hz), 7.34 (m, 3H), 7.42 (dd, 1H, J=7.8 and 4.8 Hz), 7.73 (d, 1H, J=8.7 Hz), 7.86 (d, 1H, J=8.1 Hz), 7.92 (s, 1H), 8.07 (d, 1H, J=2.1 Hz), 8.49 (dd, 1H, J=4.8 and 1.6 Hz), 8.64 (d, 1H, J=1.8 Hz), 10.60 (s, 1H, NH), 12.41 (s, 1H, NH); ESI-MS *m/z*515 [M+Na]⁺. HRMS (ESI) *m/z* calcd $C_{24}H_{21}N_4OSBrNa$ [M+Na]⁺ 515.0517 found 515.0542.

***N'*-(4-Methylthiophenyl)-*N*-[(6-methyl-2-oxo-1,2-dihydro-3-quinolinyl)methyl]-*N*-(3-pyridinylmethyl)thiourea (4e)** A white solid, yield 70%; mp 220–221 °C; ¹H NMR (DMSO-d₆, 300 MHz): δ 2.37 (s, 3H), 2.49 (s, 3H), 4.67 (s, 2H), 5.21 (s, 2H), 7.28 (d, 2H, J=9.0 Hz), 7.31 (d, 1H, J=9.0 Hz), 7.35–7.46 (m, 4H), 7.55 (s, 1H), 7.84 (td, 1H, J=8.1 and 1.8 Hz), 7.94 (s, 1H), 8.47 (dd, 1H, J=4.8 and 1.8 Hz), 8.61 (d, 1H, J=1.8 Hz), 11.20 (s, 1H, NH), 12.48 (s, 1H, NH); ESI-MS *m/z* 461 [M+H]⁺. HRMS (ESI) *m/z* calcd $C_{25}H_{25}N_4OS_2$ [M+H]⁺ 461.1470 found 461.1492.

***N'*-(4-Methylthiophenyl)-*N*-[(6-bromo-2-oxo-1,2-dihydro-3-quinolinyl)methyl]-*N*-(3-pyridinylmethyl)thiourea (4f)** A

pale yellow solid, yield 59%; mp 229–230 °C; ¹H NMR (DMSO-d₆, 300 MHz): δ 2.48 (s, 3H), 4.69 (s, 2H), 5.21 (s, 2H), 7.28 (d, 2H, J=8.7 Hz), 7.35 (d, 1H, J=9.0 Hz), 7.37–7.43 (m, 3H), 7.74 (dd, 1H, J=8.7 and 2.1 Hz), 7.84 (d, 1H, J=8.1 Hz), 7.93 (s, 1H), 8.07 (d, 1H, J=2.4 Hz), 8.49 (dd, 1H, J=4.8 and 1.6 Hz), 8.63 (d, 1H, J=1.8 Hz), 10.75 (s, 1H, NH), 12.50 (s, 1H, NH); ESI-MS *m/z* 547 [M+Na]⁺. HRMS (ESI) *m/z* calcd $C_{24}H_{21}N_4OS_2BrNa$ [M+Na]⁺ 547.0238 found 547.0243.

***N'*-(4-Dimethylamino-naphthalen-1-yl)-*N*-[(6-methyl-2-oxo-1,2-dihydro-3-quinolinyl)methyl]-*N*-(3-pyridinylmethyl)thiourea (4g)** A pale yellow solid, yield 50%; mp 201–202 °C; ¹H NMR (DMSO-d₆, 300 MHz): δ 2.37 (s, 3H), 2.81 (s, 6H), 4.80 (s, 2H), 5.27 (s, 2H), 7.11 (d, 1H, J=8.1 Hz), 7.28 (m, 2H), 7.36-7.51 (m, 4H), 7.55 (s, 1H), 7.86 (m, 2H), 7.88 (s, 1H), 8.17 (d, 1H, J=8.4 Hz), 8.47 (dd, 1H, J=5.1 and 1.5 Hz), 8.63 (d, 1H, J=1.6 Hz), 10.58 (s, 1H, NH), 12.13 (s, 1H, NH); ESI-MS *m/z* 530 [M+Na]⁺. HRMS (ESI) *m/z* calcd $C_{30}H_{29}N_5OSNa$ [M+Na]⁺ 530.1991 found 530.1978.

***N'*-(4-Bromophenyl)-*N*-[(6-methyl-2-oxo-1,2-dihydro-3-quinolinyl)methyl]-*N*-(3-pyridinylmethyl)thiourea (4h)** A white solid, yield 69%; mp 235–237 °C; ¹H NMR (DMSO-d₆, 300 MHz): δ 2.37 (s, 3H), 4.68 (s, 2H), 5.21 (s, 2H), 7.32 (d, 1H, J=8.4 Hz), 7.39 (dd, 1H, J=7.8 and 4.8 Hz), 7.44 (d, 1H, J=8.4 Hz), 7.45–7.58 (m, 5H), 7.82 (d, 1H, J=8.0 Hz), 7.96 (s, 1H), 8.47 (dd, 1H, J=4.8 and 1.6 Hz), 8.61 (d, 1H, J=1.8 Hz), 11.34 (s, 1H, NH), 12.31 (s, 1H, NH); ESI-MS *m/z* 515 [M+Na]⁺. HRMS (ESI) *m/z* calcd $C_{24}H_{21}N_4OSBrNa$ [M+Na]⁺ 515.0517 found 515.0540.

***N'*-(4-Bromophenyl)-*N*-[(6-bromo-2-oxo-1,2-dihydro-3-quinolinyl)methyl]-*N*-(3-pyridinylmethyl)thiourea (4i)** A pale yellow solid, yield 44%; mp 240–242 °C; ¹H NMR (DMSO-d₆, 300 MHz): δ 4.69 (s, 2H), 5.20 (s, 2H), 7.35 (d, 1H, J=8.7 Hz), 7.40 (dd, 1H, J=7.8 and 4.8 Hz), 7.46 (d, 2H, J=9.0 Hz), 7.55 (d, 2H, J=9.0 Hz), 7.73 (dd, 1H, J=8.7 and 2.1 Hz), 7.84 (d, 1H, J=8.1 Hz), 7.94 (s, 1H), 8.06 (d, 1H, J 2.1 Hz), 8.48 (dd, 1H, J=4.8 and 1.5 Hz), 8.61 (d, 1H, J=1.8 Hz), 10.90 (s, 1H, NH), 12.50 (s, 1H, NH); ESI-MS *m/z* 579 [M+Na]⁺. HRMS (ESI) *m/z* calcd $C_{23}H_{18}N_4OSBr_2Na$ [M+Na]⁺ 578.9466 found 578.9486.

***N'*-(3-Methoxyphenyl)-*N*-[(6-methyl-2-oxo-1,2-dihydro-3-quinolinyl)methyl]-*N*-(3-pyridinylmethyl)thiourea (4j)** A white solid, yield 65%; mp 207–209 °C; ¹H NMR (DMSO-d₆, 300 MHz): δ 2.37 (s, 3H), 3.75 (s, 3H), 4.66 (s, 2H), 5.20 (s, 2H), 6.72 (d, 1H, J=8.1 Hz), 7.10 (d, 1H, J=8.1 Hz), 7.18 (t, 1H, J=2.2 Hz, 2-Ph-H), 7.27 (t, 1H, J=7.8 Hz, 5-Ph-H), 7.31 (d, 1H, J=8.4 Hz), 7.38 (dd, 1H, J=7.8 and 4.8 Hz), 7.43 (dd, 1H, J=8.4 and 1.8 Hz), 7.54 (s, 1H), 7.82 (d, 1H, J=8.1 Hz), 7.96 (s, 1H), 8.46 (dd, 1H, J=4.8 and 1.5 Hz), 8.61 (d, 1H, J=1.8 Hz), 11.32 (s, 1H, NH), 12.35 (s, 1H, NH); ESI-MS *m/z* 467 [M+Na]⁺. HRMS (ESI) *m/z* calcd $C_{25}H_{24}N_4O_2SNa$ [M+Na]⁺ 467.1518 found 467.1500.

***N'*-(3-Methoxyphenyl)-*N*-[(6-bromo-2-oxo-1,2-dihydro-3-quinolinyl)methyl]-*N*-(3-pyridinylmethyl)thiourea (4k)** A white solid, yield 34%; mp 214–216 °C; ¹H NMR (DMSO-d₆, 300 MHz): δ 3.76 (s, 3H), 4.67 (s, 2H), 5.19 (s, 2H), 6.74 (d, 1H, J=8.4 Hz), 7.08 (d, 1H, J=8.1 Hz), 7.15 (t, 1H, J=2.1 Hz, 2-Ph-H), 7.27 (t, 1H, J=8.1 Hz, 5-Ph-H), 7.37 (d, 1H, J=8.7 Hz), 7.40 (dd, 1H, J=8.1 and 5.1 Hz), 7.73 (dd, 1H, J=8.7 and 2.1 Hz), 7.84 (td, 1H, J=7.8 and 1.8 Hz), 7.95 (s, 1H), 8.06 (d, 1H, J=2.1 Hz), 8.47 (dd, 1H, J=4.8 and 1.8 Hz), 8.62 (d, 1H, J=1.8 Hz), 10.89 (s, 1H, NH), 12.43 (s, 1H, NH); ESI-MS *m/z* 531 [M+Na]⁺. HRMS (ESI) *m/z* calcd $C_{24}H_{21}N_4O_2SBrNa$ [M+Na]⁺ 531.0466 found 531.0488.

Methyl 2-[*N'*-(6-methyl-2-oxo-1,2-dihydroquinolin-3-ylmethyl)-*N'*-pyridin-3-ylmethyl-thioureido]benzoate (4l) A white solid, yield 56%; mp 197–199 °C; ^{1}H NMR (DMSO-d$_6$, 300 MHz): δ 2.37 (s, 3H), 3.74 (s, 3H), 4.71 (s, 2H), 5.19 (s, 2H), 7.32 (m, 2H), 7.42 (m, 2H), 7.48 (d, 1H, J=7.5 Hz), 7.60 (m, 2H), 7.80 (dd, 1H, J=7.8 and 1.5 Hz), 7.88 (m, 2H), 8.50 (dd, 1H, J=4.8 and 1.5 Hz), 8.64 (d, 1H, J=1.8 Hz), 10.82 (s, 1H, NH), 12.13 (s, 1H, NH); ESI-MS *m/z* 473 [M+H]$^+$. HRMS-(ESI) *m/z* calcd C$_{26}$H$_{25}$N$_4$O$_3$S [M+H]$^+$ 473.1647 found 473.1643.

ature *N'*-(2,4-Dichlorophenyl)-*N*-[(6-methyl-2-oxo-1,2-dihydro-3-quinolinyl)methyl]-*N*-(3-pyridinylmethyl)thiourea (4m) A white solid, yield 54%; mp 235–237 °C; ^{1}H NMR (DMSO-d$_6$, 300 MHz): δ 2.37 (s, 3H), 4.71 (s, 2H), 5.22 (s, 2H), 7.29 (d, 1H, J=8.4 Hz), 7.37–7.44 (m, 4H), 7.50 (s, 1H), 7.67 (d, 1H, J=2.0 Hz), 7.84 (m, 2H), 8.49 (dd, 1H, J=4.8 and 1.5 Hz), 8.62 (d, 1H, J=1.8 Hz), 10.50 (s, 1H, NH), 12.32 (s, 1H, NH); ESI-MS *m/z* 505 [M+Na]$^+$. HRMS (ESI) *m/z* calcd C$_{24}$H$_{20}$N$_4$OSCl$_2$Na [M+Na]$^+$ 505.0633 found 505.0616.

***N'*-(4-Trifluoromethylphenyl)-*N*-[(6-methyl-2-oxo-1,2-dihydro-3-quinolinyl)methyl]-*N*-(3-pyridinylmethyl)thiourea (4n)** A white solid, yield 65%; mp 231–233 °C; ^{1}H NMR (DMSO-d$_6$, 300 MHz): δ 2.39 (s, 3H), 4.70 (s, 2H), 5.21 (s, 2H), 7.33 (d, 1H, J=8.4 Hz), 7.39 (dd, 1H, J=7.8 and 4.8 Hz), 7.45 (d, 1H, J=7.8 Hz), 7.56 (s, 1H), 7.77–7.83 (m, 5H), 8.02 (s, 1H), 8.47 (dd, 1H, J=4.8 and 2.0 Hz), 8.62 (d, 1H, J=1.8 Hz), 11.50 (s, 1H, NH), 12.62 (s, 1H, NH); ESI-MS *m/z* 505 [M+Na]$^+$. HRMS (ESI) *m/z* calcd C$_{25}$H$_{21}$N$_4$OSF$_3$Na [M+Na]$^+$ 505.1286 found 505.1287.

***N'*-(Naphthalen-1-yl)-*N*-[(6-methyl-2-oxo-1,2-dihydro-3-quinolinyl)methyl]-*N*-(3-pyridinylmethyl)thiourea (4o)** A white solid, yield 55%; mp 219–221 °C; ^{1}H NMR (DMSO-d$_6$, 300 MHz): δ 2.39 (s, 3H), 4.84 (s, 2H), 5.30 (s, 2H), 7.31 (d, 1H, J=8.4 Hz), 7.39–7.58 (m, 7H), 7.85 (d, 1H, J=8.1 Hz), 7.90 (d, 1H, J=8.1 Hz), 7.97 (m, 3H), 8.50 (dd, 1H, J=4.8 and 1.5 Hz), 8.66 (d, 1H, J=1.8 Hz), 10.76 (s, 1H, NH), 12.35 (s, 1H, NH); ESI-MS *m/z* 487 [M+Na]$^+$. HRMS (ESI) *m/z* calcd C$_{28}$H$_{24}$N$_4$OSNa [M+Na]$^+$ 487.1569 found 487.1548.

***N'*-(Naphthalen-1-yl)-*N*-[(6-bromo-2-oxo-1,2-dihydro-3-quinolinyl)methyl]-*N*-(3-pyridinylmethyl)thiourea (4p)** A white solid, yield 55%; mp 219–221 °C; ^{1}H NMR (DMSO-d$_6$, 300 MHz): δ 4.85 (s, 2H), 5.30 (s, 2H), 7.34 (d, 1H, J=8.7 Hz), 7.42–7.57 (m, 5H), 7.73 (dd, 1H, J=8.7 and 2.4 Hz), 7.86 (d, 1H, J=8.1 Hz), 7.88–7.97 (m, 4H), 8.12 (d, 1H, J=2.4 Hz), 8.52 (dd, 1H, J=4.8 and 1.5 Hz), 8.68 (d, 1H, J=1.8 Hz), 10.33 (s, 1H, NH), 12.20 (s, 1H, NH); ESI-MS *m/z* 551 [M+Na]$^+$. HRMS (ESI) *m/z* calcd C$_{27}$H$_{21}$N$_4$OSBrNa [M+Na]$^+$ 551.0517 found 551.0514.

***N'*-(3-Trifluoromethylphenyl)-*N*-[(6-methyl-2-oxo-1,2-dihydro-3-quinolinyl)methyl]-*N*-(3-pyridinylmethyl)thiourea (4q)** A white solid, yield 63%; mp 221–223 °C; ^{1}H NMR (DMSO-d$_6$, 300 MHz): δ 2.37 (s, 3H), 4.70 (s, 2H), 5.21 (s, 2H), 7.33 (d, 1H, J=8.4 Hz), 7.41 (dd, 1H, J=7.8 and 4.8 Hz), 7.45 (dd, 1H, J=8.4 and 1.8 Hz), 7.48 (d, 1H, J=8.1 Hz), 7.61 (m, 2H), 7.80–7.89 (m, 3H), 8.00 (s, 1H), 8.47 (dd, 1H, J=4.8 and 1.5 Hz), 8.62 (d, 1H, J=1.8 Hz), 11.76 (s, 1H, NH), 12.43 (s, 1H, NH); ESI-MS *m/z* 505 [M+Na]$^+$. HRMS (ESI) *m/z* calcd C$_{25}$H$_{21}$N$_4$OSF$_3$Na [M+Na]$^+$ 505.1286 found 505.1252.

***N'*-(3-Trifluoromethylphenyl)-*N*-[(6-bromo-2-oxo-1,2-dihydro-3-quinolinyl)methyl]-*N*-(3-pyridinylmethyl)thiourea (4r)** A pale yellow solid, yield 33%; mp 221–222 °C; ^{1}H NMR (DMSO-

d$_6$, 300 MHz): δ 4.71 (s, 2H), 5.20 (s, 2H), 7.35 (d, 1H, J=8.7 Hz), 7.41 (dd, 1H, J=8.1 and 4.8 Hz), 7.49 (d, 1H, J=7.5 Hz), 7.62 (t, 1H, J=7.8 Hz), 7.75 (dd, 1H, J=8.7 and 2.4 Hz), 7.86 (m, 3H), 7.99 (s, 1H), 8.08 (d, 1H, J=2.4 Hz), 8.49 (dd, 1H, J=4.8 and 1.5 Hz), 8.64 (d, 1H, J=1.8 Hz), 10.70 (s, 1H, NH), 12.35 (s, 1H, NH); ESI-MS *m/z* 569 [M+Na]$^+$. HRMS (ESI) *m/z* calcd C$_{24}$H$_{18}$N$_4$OSBrF$_3$Na [M+Na]$^+$ 569.0234 found 569.0231.

***N'*-(3,4-Dichlorophenyl)-*N*-[(6-methyl-2-oxo-1,2-dihydro-3-quinolinyl)methyl]-*N*-(3-pyridinylmethyl)thiourea (4s)** A white solid, yield 55%; mp 237–239 °C; ^{1}H NMR (DMSO-d$_6$, 300 MHz): δ 2.37 (s, 3H), 4.68 (s, 2H), 5.19 (s, 2H), 7.32 (d, 1H, J=8.4 Hz), 7.39 (dd, 1H, J=7.8 and 4.8 Hz), 7.44 (dd, 1H, J=8.4 and 1.5 Hz), 7.56 (m, 2H), 7.63 (d, 1H, J=8.4 Hz), 7.83 (m, 2H), 7.99 (s, 1H), 8.47 (dd, 1H, J=4.8 and 1.5 Hz), 8.61 (d, 1H, J=1.8 Hz), 11.74 (s, 1H, NH), 12.56 (s, 1H, NH); ESI-MS *m/z* 505 [M+Na]$^+$. HRMS (ESI) *m/z* calcd C$_{24}$H$_{20}$N$_4$OSCl$_2$Na [M+Na]$^+$ 505.0633 found 505.0636.

***N'*-(3,4-Dichlorophenyl)-*N*-[(6-bromo-2-oxo-1,2-dihydro-3-quinolinyl)methyl]-*N*-(3-pyridinylmethyl)thiourea (4t)** A pale yellow solid, yield 60%; mp 239–240 °C; ^{1}H NMR (DMSO-d$_6$, 300 MHz): δ 4.68 (s, 2H), 5.19 (s, 2H), 7.34 (d, 1H, J=9.0 Hz), 7.41 (dd, 1H, J=7.8 and 4.8 Hz), 7.52 (dd, 1H, J=8.7 and 2.4 Hz), 7.63 (d, 1H, J=8.4 Hz), 7.74 (dd, 1H, J=8.4 and 2.4 Hz), 7.85 (m, 2H), 7.97 (s, 1H), 8.07 (d, 1H, J=2.1 Hz), 8.49 (dd, 1H, J=4.8 and 1.8 Hz), 8.63 (d, 1H, J=1.8 Hz), 11.12 (s, 1H, NH), 12.47 (s, 1H, NH); ESI-MS *m/z* 547 [M+H]$^+$. HRMS (ESI) *m/z* calcd C$_{23}$H$_{18}$N$_4$OSBrCl$_2$ [M+H]$^+$ 546.9762 found 546.9775.

***N'*-(4-Nitrophenyl)-*N*-[(6-methyl-2-oxo-1,2-dihydro-3-quinolinyl)methyl]-*N*-(3-pyridinylmethyl)thiourea (4u)** A yellow solid, yield 66%; mp 258–260 °C; ^{1}H NMR (DMSO-d$_6$, 300 MHz): δ 2.37 (s, 3H), 4.72 (s, 2H), 5.19 (s, 2H), 7.34 (d, 1H, J=8.4 Hz), 7.38 (dd, 1H, J=7.8 and 4.8 Hz), 7.46 (d, 1H, J=7.8 Hz), 7.55 (s, 1H), 7.80 (d, 1H, J=7.2 Hz), 7.86 (d, 2H, J=9.3 Hz), 8.07 (s, 1H), 8.27 (d, 2H, J=9.3 Hz), 8.46 (dd, 1H, J=4.8 and 1.8 Hz), 8.60 (d, 1H, J=1.8 Hz), 10.73 (s, 1H, NH), 12.24 (s, 1H, NH); ESI-MS *m/z* 482 [M+Na]$^+$. HRMS (ESI) *m/z* calcd C$_{24}$H$_{21}$N$_5$O$_3$SNa [M+Na]$^+$ 482.1263 found 482.1290.

***N'*-(4-Nitrophenyl)-*N*-[(6-bromo-2-oxo-1,2-dihydro-3-quinolinyl)methyl]-*N*-(3-pyridinylmethyl)thiourea (4v)** A yellow solid, yield 42%; mp 257–258 °C; ^{1}H NMR (DMSO-d$_6$, 300 MHz): δ 4.72 (s, 2H), 5.19 (s, 2H), 7.40 (m, 2H), 7.77 (dd, 1H, J=8.7 and 2.4 Hz), 7.85 (m, 3H), 8.07 (d, 2H, J=2.1 Hz), 8.28 (d, 2H, J=9.0 Hz), 8.48 (dd, 1H, J=4.8 and 1.5 Hz), 8.63 (d, 1H, J=1.8 Hz), 10.23 (s, 1H, NH), 12.10 (s, 1H, NH); ESI-MS *m/z* 546 [M+Na]$^+$. HRMS (ESI) *m/z* calcd C$_{23}$H$_{18}$N$_5$O$_3$SBrNa [M+Na]$^+$ 546.0211 found 546.0184.

***N'*-(2-Fluorophenyl)-*N*-[(6-methyl-2-oxo-1,2-dihydro-3-quinolinyl)methyl]-*N*-(3-pyridinylmethyl)thiourea (4w)** An off-white solid, yield 54%; mp 222–224 °C; ^{1}H NMR (DMSO-d$_6$, 300 MHz): δ 2.37 (s, 3H), 4.71 (s, 2H), 5.22 (s, 2H), 7.16–7.28 (m, 4H), 7.35–7.40 (m, 3H), 7.50 (s, 1H), 7.83 (m, 2H), 8.48 (dd, 1H, J=4.8 and 1.5 Hz), 8.61 (d, 1H, J=1.8 Hz), 10.50 (s, 1H, NH), 12.43 (s, 1H, NH); ESI-MS *m/z* 455 [M+Na]$^+$. HRMS (ESI) *m/z* calcd C$_{24}$H$_{21}$N$_4$OSFNa [M+Na]$^+$ 455.1318 found 455.1349.

Methyl 2-{*N'*-(6-methyl-2-oxo-1,2-dihydroquinolin-3-yl-methyl)-*N'*-[2-(piperidin-1-yl)ethyl]thioureido}benzoate (5a) A pale yellow solid, yield 74%; mp 209–210 °C; ^{1}H NMR (DMSO-d$_6$, 300 MHz): δ 1.43 (m, 6H), 2.34 (s, 3H), 2.50 (m, 4H), 2.63 (m, 2H), 3.81 (m, 5H), 4.85 (s, 2H), 7.18 (m, 1H), 7.28 (m, 2H), 7.35 (t, 1H, J=7.2 Hz), 7.46 (m, 2H), 7.60 (t, 1H, J=7.2 Hz), 7.80 (t, 1H, J=7.5

Hz), 10.33 (s, 1H, NH), 12.05 (s, 1H, NH); ESI-MS *m/zz* 515 [M+Na]$^+$. HRMS (ESI) *m/z* calcd $C_{27}H_{32}N_4O_3SNa$ [M+Na]$^+$ 515.2093 found 515.2122.

Methyl (±)-2-{*N'*-[1-(ethylpyrrolidin-2-yl)methyl]-*N'*-(6-methyl-2-oxo-1,2-dihydroquinolin-3-ylmethyl)thioureido}benzoate (5b) A pale yellow solid (as a racemic mixture), yield 64%; mp 212–213 °C; ^{1}H NMR (DMSO-d_6, 300 MHz): δ 0.99 (t, 3H, J=7.2 Hz), 1.62 (m, 1H), 1.78 (m, 2H), 1.92 (m, 1H), 2.34 (s, 3H), 2.44(m, 2H), 2.84 (m, 1H), 3.06 (m, 1H), 3.16 (m, 1H), 3.68–3.83 (m, 5H), 4.74 (d, 1H, J=17.1 Hz, aryl-CHN), 5.08 (d, 1H, J=17.1 Hz, aryl-CHN), 7.26 (m, 3H), 7.33 (d, 1H, J=8.4 Hz), 7.44 (s, 1H), 7.57 (t, 1H, J=7.8 Hz), 7.69 (s, 1H), 7.75 (d, 1H, J=8.1 Hz), 11.90 (s, 1H, NH), 13.05 (s, 1H, NH); ESI-MS *m/z* 515 [M+Na]$^+$. HRMS (ESI) *m/z* calcd $C_{27}H_{32}N_4O_3SNa$ [M+Na]$^+$ 515.2093 found 515.2047.

Methyl 2-{*N'*-[2-(indol-3-yl)ethyl]-*N'*-(6-methyl-2-oxo-1,2-dihydroquinolin-3-ylmethyl)thioureido}benzoate (5c) A yellow solid, yield 67%; mp 192–194 °C; ^{1}H NMR (DMSO-d_6, 300 MHz): δ 2.33 (s, 3H), 3.21 (t, 2H, J=7.2 Hz), 3.74 (s, 3H), 4.05 (t, 2H, J=7.2 Hz), 4.82 (s, 2H), 6.98 (t, 1H, J=7.5 Hz), 7.08 (t, 1H, J=7.5 Hz), 7.21–7.36 (m, 6H), 7.47 (s, 1H), 7.58 (t, 1H, J=8.4 Hz), 7.67 (d, 1H, J=7.8 Hz), 7.79 (m, 2H), 11.20 (s, 1H, NH), 12.54 (s, 1H, NH); ESI-MS *m/z* 547 [M+Na]$^+$. HRMS (ESI) *m/z* calcd $C_{30}H_{28}N_4O_3SNa$ [M+Na]$^+$ 547.1780 found 547.1788.

Methyl 2-[N'-benzyl-N'-(6-methyl-2-oxo-1,2-dihydroquinolin-3-ylmethyl)thioureido]benzoate (5d) A pale yellow solid, yield 65%; mp 209–211 °C; ^{1}H NMR (DMSO-d_6, 300 MHz): δ 2.35 (s, 3H), 3.73 (s, 3H), 4.68 (s, 2H), 5.16 (s, 2H), 7.30 (t, 3H, J=7.2 Hz), 7.44 (m, 5H), 7.57 (m, 3H), 7.79 (m, 2H), 10.56 (s, 1H, NH), 12.30 (s, 1H, NH); ESI-MS *m/z* 494 [M+Na]$^+$. HRMS (ESI) *m/z* calcd $C_{27}H_{25}N_3O_3SNa$ [M+Na]$^+$ 494.1514 found 494.1526.

Methyl 2-[*N'*-(2-chlorobenzyl)-*N'*-(6-methyl-2-oxo-1,2-dihydroquinolin-3-ylmethyl)thioureido]benzoate (5e) An off-white solid, yield 48%; mp 211–213 °C; ^{1}H NMR (DMSO-d_6, 300 MHz): δ 2.35 (s, 3H), 3.75 (s, 3H), 4.77 (s, 2H), 5.15 (s, 2H), 7.25–7.38 (m, 6H), 7.45–7.57 (m, 4H), 7.79 (d, 1H, J=7.5 Hz), 7.86 (s, 1H), 10.42 (s, 1H, NH), 12.47 (s, 1H, NH); ESI-MS *m/z* 528 [M+Na]$^+$. HRMS (ESI) *m/z* calcd $C_{27}H_{24}N_3O_3SClNa$ [M+Na]$^+$ 528.1125 found 528.1085.

Methyl 2-[*N'*-(6-methyl-2-oxo-1,2-dihydroquinolin-3-ylmethyl)-*N'*-(thiophen-2-ylmethyl)thioureido]benzoate (5f) A pale yellow solid, yield 52%; mp 203–205 °C; ^{1}H NMR (DMSO-d_6, 300 MHz): δ 2.37 (s, 3H), 3.66 (s, 3H), 4.68 (s, 2H), 5.27 (s, 2H), 7.02 (dd, 1H, J=5.1 and 3.6 Hz), 7.31 (m, 3H), 7.41 (dd, 1H, J=8.4 and 1.5 Hz), 7.48 (dd, 1H, J=5.1 and 1.2 Hz), 7.57 (m, 3H), 7.79 (dd, 1H, J=8.4 and 1.5 Hz), 7.85 (s, 1H), 10.38 (s, 1H, NH), 12.56 (s, 1H, NH); ESI-MS *m/z* 500 [M+Na]$^+$. HRMS (ESI) *m/z* calcd $C_{25}H_{23}N_3O_3S_2Na$ [M+Na]$^+$ 500.1079 found 500.1109.

Methyl 2-[*N'*-(furan-2-ylmethyl)-*N'*-(6-methyl-2-oxo-1,2-dihydroquinolin-3-ylmethyl)thioureido]benzoate (5g) A pale yellow solid, yield 68%; mp 206–208 °C; ^{1}H NMR (DMSO-d_6, 300 MHz): δ 2.35 (s, 3H), 3.67 (s, 3H), 4.80 (s, 2H), 5.14 (s, 2H), 6.49 (m, 2H), 7.30 (m, 2H), 7.34 (d, 1H, J=7.1 Hz), 7.49 (s, 1H), 7.61 (m, 3H), 7.70 (s, 1H), 7.80 (d, 1H, J=7.8 Hz), 10.50 (s, 1H, NH), 12.84 (s, 1H, NH); ESI-MS *m/z* 484 [M+Na]$^+$. HRMS (ESI) *m/z* calcd $C_{25}H_{23}N_3O_4SNa$ [M+Na]$^+$ 484.1307 found 484.1338.

Methyl 2-[*N'*-(2,3-dihydrobenzo[1,4]dioxin-6-ylmethyl)-*N'*-(6-methyl-2-oxo-1,2-dihydroquinolin-3-ylmethyl)thioureido]benzoate (5h) A white solid, yield 38%; mp 97–99 °C; ^{1}H

NMR (CDCl$_3$, 300 MHz): δ 2.40 (s, 3H), 3.67 (s, 3H), 4.24 (s, 4H), 5.00 (s, 2H), 5.22 (s, 2H), 6.85 (d, 1H, J=8.4 Hz), 6.93 (d, 1H, J=8.4 Hz), 6.98 (s, 1H), 7.12 (t, 1H, J=7.8 Hz), 7.19 (d, 1H, J=8.7 Hz), 7.30 (d, 1H, J=7.8 Hz), 7.37 (s, 1H), 7.53 (t, 1H, J=7.8 Hz), 7.70 (s, 1H), 7.89 (d, 1H, J=7.5 Hz), 8.57 (d, 1H, J=8.1 Hz), 10.92 (s, 1H, NH), 11.08 (s, 1H, NH); ESI-MS *m/z* 552 [M+Na]$^+$. HRMS (ESI) *m/z* calcd $C_{29}H_{27}N_3O_5SNa$ [M+Na]$^+$ 552.1569 found 552.1533.

References

1   Aaronson SA. Growth factors and cancer. Science 1991; 254: 1146–52.
2   Bridges AJ. Chemical inhibitors of protein kinases. Chem Rev 2001; 101: 2541–72.
3   Ullrich A, Schlessinger J. Signal transduction by receptors with tyrosine kinase activity. Cell 1990; 61: 203–12.
4   Elder JT, Fisher GJ, Lindquist PB, Bennett GL, Pittelkow MR, Coffey RJ, *et al*. Overexpression of transforming growth factor alpha in psoriatic epidermis. Science 1989; 243: 811–4.
5   Yang EB, Guo YJ, Zhang K, Chen YZ, Mack P. Inhibition of epidermal growth factor receptor tyrosine kinase by chalcone derivatives. Biochim Biophys Acta 2001; 1550: 144–52.
6   Traxler P, Bold G, Buchdunger E, Caravatti G, Furet P, Manley P, *et al*. Tyrosine kinase inhibitors: from rational design to clinical trials. Med Res Rev 2001; 21: 499–512.
7   Traxler P, Bold G, Frei J, Lang M, Lydon N, Mett H, *et al*. Use of a pharmacophore model for the design of EGF-R tyrosine kinase inhibitors: 4-(phenylamino)pyrazolo[3,4-d]pyrimidines. J Med Chem 1997; 40: 3601–16.
8   Khazaie K, Shirrmacher V, Lichtner RB. EGF receptor in neoplasia and metastasis. Cancer Metast Rev 1993; 12: 155–274.
9   Fry DW, Kraker AJ, McMichael A, Ambroso LA, Nelson JM, Leopold WR, *et al*. A specific inhibitor of the epidermal growth factor receptor tyrosine kinase. Science 1994; 265: 1093–5.
10 Chinkers M, Brugge JS. Characterization of structural domains of the human epidermal growth factor receptor obtained by partial proteolysis. J Biol Chem 1984; 259: 11 534–42.
11 Carpenter CD, Ingraham HA, Cochet C, Walton GM, Lazar CS, Sowadski JM, *et al*. Structural analysis of the transmembrane domain of the epidermal growth factor receptor. J Biol Chem 1991; 266: 5750–5.
12 Araujo RP, Petricoin EF, Liotta LA. A mathematical model of combination therapy using the EGFR signaling network. Biosystems 2005; 80: 57–9.
13 Wissner A, Overbeek E, Reich MF, Floyd MB, Johnson BD, Mamuya N, *et al*. Synthesis and structure-activity relationships of 6,7-disubstituted 4-anilinoquinoline-3-carbonitriles. The design of an orally active, irreversible inhibitor of the tyrosine kinase activity of the epidermal growth factor receptor (EGFR) and the human epidermal growth factor receptor-2 (HER-2). J Med Chem 2003; 46: 49–63.
14 Tsou HR, Mamuya N, Johnson BD, Reich MF, Gruber BC, Ye F, *et al*. 6-Substituted-4-(3-bromophenylamino) quinazolines as putative irreversible inhibitors of the epidermal growth factor receptor (EGFR) and human epidermal growth factor receptor (HER-2) tyrosine kinases with enhanced antitumor activity. J Med Chem 2001; 44: 2719–34.
15 Mu F, Coffing SL, Riese DJ, Geahlen RL, Verdier-Pinard P, Hamel

TE, *et al*. Design, synthesis, and biological evaluation of a series of lavendustin A analogues that inhibit EGFR and Syk tyrosine kinases, as well as tubulin polymerization. J Med Chem 2001; 44: 441–52.

16 Jin Y, Li HY, Lin LP, Tan J, Ding J, Luo X, *et al*. Synthesis and antitumor evaluation of novel 5-substituted-4-hydroxy-8-nitroquinazolines as EGFR signaling-targeted inhibitors. Bioorg Med Chem 2005; 13: 5613–22.

17 Albuschat R, Löwe W, Weber M, Luger P, Jendrossek V. 4-Anilinoquinazolines with lavendustin A subunit as inhibitors of epidermal growth factor receptor tyrosine kinase: syntheses, chemical and pharmacological properties. Eur J Med Chem 2004; 39: 1001–11.

18 Asano T, Yoshikawa T, Usui T, Yamamoto H, Yamamoto Y, Uehara Y, *et al*. Benzamides and benzamidines as specific inhibitors of epidermal growth factor receptor and v-Src protein tyrosine kinases. Bioorg Med Chem 2004; 12: 3529–42.

19 Supuran CT, Scozzafava A. Protein tyrosine kinase inhibitors as anticancer agents. Expert Opin Ther Patents 2004; 14: 35–53.

20 Chen G, Luo X, Zhu W, Luo C, Liu H, Puah CM, *et al*. Elucidating inhibitory models of the inhibitors of epidermal growth factor receptor by docking and 3D-QSAR. Bioorg Med Chem 2004; 12: 2409–17.

21 Norman P. ZD-1839 (astraZeneca). Curr Opin Investig Drugs 2001; 3: 428–34.

22 Norman P. OSI-774 OSI pharmaceuticals. Curr Opin Investig Drugs 2001; 2: 298–304.

23 Smaill JB, Palmer BD, Rewcastle GW, Denny WA, McNamara DJ, Dobrusin EM, *et al*. Tyrosine kinase inhibitors. 15. 4-(phenylamino)quinazoline and 4-(phenylamino)pyrido[d]pyrimidine acrylamides as irreversible inhibitors of the ATP binding site of the epidermal growth factor receptor. J Med Chem 1999; 42: 1803–15.

24 Fry DW, Bridges AJ, Denny WA, Doherty A, Greis KD, Hicks JL, *et al*. Specific, irreversible inactivation of the epidermal growth factor receptor and erbB2, by a new class of tyrosine kinase inhibitor. Proc Natl Acad Sci USA 1998; 95: 12022–7.

25 Wissner A, Johnson BD, Floyd MB, Kitchen DB, inventors; American Cyanamid Company, assignee. 4-Aminoquinazolines as EGFR inhibitors. US Patent 5 760 041. 1998; Jun 2.

26 Lee MW, Seo CW, Kim SW, Yang HJ, Lee HW, Choi JH, *et al*. Cutaneous side effects in non-small cell lung cancer patients treated with Iressa (ZD1839), an inhibitor of epidermal growth factor. Acta Derm Venereol 2004; 84: 23–6.

27 Kuntz ID, Meng EC, Shoichet BK. Receptor-based molecular design. Acc Chem Res 1994; 27: 117–23.

28 Wang JL, Liu D, Zhang ZJ, Shan S, Han X, Srinivasula SM, *et al*. Structure-based discovery of an organic compound that binds Bcl-2 protein and induces apoptosis of tumor cells. Proc Natl Acad Sci USA 2000; 97: 7124–9.

29 Liu H, Li Y, Song M, Tan X, Cheng F, Zheng S, *et al*. Structure-based discovery of potassium channel blockers from natural products: Virtual screening and electrophysiological assay testing. Chem Biol 2003; 10: 1103–13.

30 Stamos J, Sliwkowski MX, Eigenbrot C. Structure of the epidermal growth factor receptor kinase domain alone and in complex with a 4-anilinoquinazoline inhibitor. J Biol Chem 2002; 277:

46 265–72.

31 Li J, Chen J, Gui C, Zhang L, Qin Y, Xu Q, *et al*. Discovering novel chemical inhibitors of human cyclophilin A: virtual screening, synthesis, and bioassay. Bioorg Med Chem 2006; 14: 2209–24.

32 Ewing T, Kuntz ID. Critical evaluation of search algorithms used in automated molecular docking. J Comput Chem 1997; 18: 1175–89.

33 Kuntz ID. Structure-based strategies for drug design and discovery. Science 1992; 257: 1078–82.

34 Weiner SJ, Kollman PA, Nguyen DT, Case DA. An all atom force field for simulations of proteins and nucleic acids. J Comput Chem 1986; 7: 230–52.

35 Gasteiger J, Marsili M. Iterative partial equalization of orbital electronegativity-A rapid access to atomic charges. Tetrahedron 1980; 36: 3219–28.

36 Muegge I, Rarey M. Small molecule docking and scoring. In: Lipkowitz KB, Boyd DB, editors. Reviews in computational chemistry.. New York: John Wiley & Sons; 2001. p 1–60.

37 Charifson PS, Corkery JJ, Murcko MA, Walters WP. Consensus scoring: a method for obtaining improved hit rates from docking databases of three-dimensional structures into proteins. J Med Chem 1999; 42: 5100–9.

38 Sybyl molecular modeling package (Computer program). Version 6.8. St Louis, MO: Tripos Associates, 2000.

39 Traxler P, Furet P, Mett H, Buchdunger E, Meyer T, Lydon N. Design and synthesis of novel tyrosine kinase inhibitors using a pharmacophore model of the ATP-binding site of the EGF-R. J Pharm Belg 1997; 52: 88–96.

40 Meth-Cohn O, Narine B, Tarnowski B. A versatile new synthesis of quinolines and related fused pyridines. Part 5. The synthesis of 2-chloroquinoline-3-carbaldehydes. J Chem Soc Perkin Trans 1 1981; 5: 1520–30.

41 Meth-Cohn O, Narine B, Tarnowski B, Hayes R, Keyzad A, Rhouati S, *et al*. A versatile new synthesis of quinolines and related fused pyridines. Part 9. Synthetic application of the 2-chloroquinoline-3-carbaldehydes. J Chem Soc Perkin Trans 1 1981; 9: 2509–17.

42 Tilakraj T, Ambekar SY. Synthesis and mass spectra of some 2H-pyrano[2,3-b]quinolin-2-ones. J Indian Chem Soc 1985; 62: 251–3.

43 Guo XN, Zhong L, Zhang XH, Zhao WM, Zhang XW, Lin LP, *et al*. Evaluation of active recombinant catalytic domain of human ErbB-2 tyrosine kinase, and suppression of activity by a naturally derived inhibitor, ZH-4B. Biochim Biophys Acta 2004; 1673: 186–93.

44 Sargent JM, Taylor CG. Appraisal of the MTT assay as a rapid test of chemosensitivity in acute myeloid leukaemia. Br J Cancer 1989; 60: 206–10.

45 Rewcastle GW, Denny WA, Bridges AJ, Zhou H, Cody DR, McMichael A, *et al*. Tyrosine kinase inhibitors. 5. Synthesis and structure-activity relationships for 4-[(phenylmethyl)amino]- and 4-(phenylamino)quinazolines as potent adenosine 5'-triphosphate binding site inhibitors of the tyrosine kinase domain of the epidermal growth factor receptor. J Med Chem 1995; 38: 3482–7.